OXFORD

SOT | Society of Toxicology
www.toxsci.oxfordjournals.org

*TOXICOLOGICAL SCIENCES*, 144(2), 2015, 366–381

doi: 10.1093/toxsci/kfv005
Advance Access Publication Date: January 9, 2015

# Influence of Particle Size on Persistence and Clearance of Aerosolized Silver Nanoparticles in the Rat Lung

Donald S. Anderson*, Esther S. Patchin*, Rona M. Silva*, Dale L. Uyeminami*, Arjun Sharmah†, Ting Guo†, Gautom K. Das‡, Jared M. Brown§, Jonathan Shannahan§, Terry Gordon¶, Lung Chi Chen¶, Kent E. Pinkerton*,||,|||, and Laura S. Van Winkle*,||,1

*Center for Health and the Environment, †Department of Chemistry, ‡Department of Mechanical and Aerospace Engineering, University of California Davis, Davis, California 95616, §Skaggs School of Pharmacy and Pharmaceutical Sciences, University of Colorado, Anschutz Medical Campus, Aurora, Colorado 80045, ¶Department of Environmental Medicine, Langone Medical Center, New York University, Tuxedo, New York 10987, ||Department of Anatomy, Physiology and Cell Biology, School of Veterinary Medicine, University of California Davis, Davis, California 95616 and |||Department of Pediatrics, School of Medicine, University of California Davis, Sacramento, California 95817

[1]To whom correspondence should be addressed at Department of Anatomy, Physiology and Cell Biology, School of Veterinary Medicine, University of California Davis, One Shields Avenue, Davis, California 95616. Tel: 530-754-7547; Fax: 530-752-5300; E-mail: lsvanwinkle@ucdavis.edu.

Downloaded from http://toxsci.oxfordjournals.org/ at Government on August 9, 2016

## ABSTRACT

The growing use of silver nanoparticles (AgNPs) in consumer products raises concerns about potential health effects. This study investigated the persistence and clearance of 2 different size AgNPs (20 and 110 nm) delivered to rats by single nose-only aerosol exposures (6 h) of 7.2 and 5.4 mg/m$^3$, respectively. Rat lung tissue was assessed for silver accumulations using inductively-coupled plasma mass spectrometry (ICP-MS), autometallography, and enhanced dark field microscopy. Involvement of tissue macrophages was assessed by scoring of silver staining in bronchoalveolar lavage fluid (BALF). Silver was abundant in most macrophages at 1 day post-exposure. The group exposed to 20 nm AgNP had the greatest number of silver positive BALF macrophages at 56 days post-exposure. While there was a significant decrease in the amount of silver in lung tissue at 56 days post-exposure compared with 1 day following exposure, at least 33% of the initial delivered dose was still present for both AgNPs. Regardless of particle size, silver was predominantly localized within the terminal bronchial/alveolar duct junction region of the lung associated with extracellular matrix and within epithelial cells. Inhalation of both 20 and 110 nm AgNPs resulted in a persistence of silver in the lung at 56 days post-exposure and local deposition as well as accumulation of silver at the terminal bronchiole alveolar duct junction. Further the smaller particles, 20 nm AgNP, produced a greater silver burden in BALF macrophages as well as greater persistence of silver positive macrophages at later timepoints (21 and 56 days).

**Key words**: lung; inhaled; engineered nanomaterials; inhalation; macrophage

Silver nanoparticles (AgNPs) have antimicrobial activity and are used in wound dressings, sprays, textiles, and medical devices (Pelgrift and Friedman, 2013). Silver nanomaterials are found in 50% of the products known to contain nanomaterials (The Project of Emerging Nanotechnologies, 2014). While most inhalation exposures to silver nanomaterials are thought to occur as occupational exposures during manufacturing (Lee *et al.*, 2012), the use of colloidal silver in wound sprays and silver iodide particles as ground-based aerosols for cloud seeding underscores the need to gain a better understanding of how silver nanomaterials persist in the body, especially the lung. Further, silver nanomaterials are an area of active

© The Author 2015. Published by Oxford University Press on behalf of the Society of Toxicology.
All rights reserved. For Permissions, please e-mail: journals.permissions@oup.com

investigation of inhalable therapies for respiratory infections (Hindi *et al.*, 2009; Xiang *et al.*, 2013) and allergic airway inflammation (Jang *et al.*, 2012).

Previous work on the distribution of inhaled AgNPs in the respiratory system primarily examines a single nanoparticle size and involved subacute or subchronic exposures. One group, in a series of experiments, exposed rats in whole body chambers to 18 nm uncoated AgNP for 28 days (Ji *et al.*, 2007) or 90 days (Sung *et al.*, 2008, 2009) and quantified silver deposition in the lung using atomic absorption spectrometry. However, only the accumulated amount of AgNPs in the lung at the end of the repeated exposure was determined; persistence of silver in the lung after a single dose was not investigated. While several previous studies show persistence of silver in the lungs of mice and/or rats (Braakhuis *et al.*, 2014; Kwon *et al.*, 2012; Stebounova *et al.*, 2011; Takenaka *et al.*, 2001), at least one previous study has also found substantial clearance over 1–7 days following exposure (Braakhuis *et al.*, 2014), see summary Table 1. Very recently a comparative study was published on 15 and 410 nm spark generated silver particles that were given 6 h per day for 4 consecutive days in rats (Braakhuis *et al.*, 2014). Analysis of silver in the rat lungs from this study showed a significant reduction in silver content between 1 and 7 days after the end of the exposure cycle. What is common about these studies is the use of a single size of AgNP, primarily smaller than 20 nm, which can affect the clearance of particles from the lung (Oberdorster *et al.*, 1994). These studies all indicate that silver, in some form, persisted in the lung at the latest timepoint tested, and found no signs of toxicity and only mild inflammation. Comparative analysis of the amount of silver retention in lung tissues for a single exposure to inhaled AgNPs of different sizes, and as a percentage of the delivered dose immediately at the end of exposure, has not been reported.

One mechanism of removal of lung-deposited particles can be uptake by inflammatory cells. Macrophages are the predominant inflammatory phagocytic cell type that is resident and recruited to the lung, often comprising 98% or more of the cells obtained in bronchoalveolar lavage. Hence, when studying long-term clearance of nanoparticles from lung tissue, assessment of macrophage involvement is key to fully understanding the response. Our current study expands the literature on inhaled nanosilver because we study clearance from the rat lung over time while comparing 2 particle sizes following a single nose-only inhalation exposure.

In this study, we describe development and characterization of an exposure system for aerosolization of AgNPs and we examine 2 different sizes of aerosolized AgNPs in the exposure system and in the lung. Citrate-coated particles were selected because previous work showed that these were the most persistent in lung tissue and created the greatest biological response in terms of persistence of the particles in the lung within the lung macrophage population (Anderson *et al.*, 2014). The goals of this study were: (1) to define AgNP persistence in the lung tissue and lung macrophage population following an inhalation exposure to well-characterized nanomaterials and (2) to compare results with a previous study using the same nanomaterials given by a different route, instillation.

## MATERIALS AND METHODS

*Silver nanoparticles*. AgNPs manufactured by nanoComposix, Inc (San Diego, California) were supplied by the NIEHS Centers for Nanotechnology Health Implications Research (NCNHIR) Consortium. Preliminary testing and characterization of the materials were performed by the Nanotechnology Characterization Laboratory (SAIC-Fredrick, Frederick, Maryland) (Wang *et al.*, 2014). AgNPs consisted of 2 sizes 20 and 110 nm and were stabilized in citrate. AgNPs were supplied in sealed 50 ml aliquots at 1.0 mg/ml. The sham control was 2mM citrate buffer (pH 7.5), at the same concentration used for the AgNP suspensions, so that effects of the buffer could be separated from AgNP effects. Citrate buffer was prepared using sodium citrate and citrate acid (Sigma) in endotoxin-free water (Fisher Scientific, Pittsburgh, Pennsylvania).

*Exposure system*. Exposures were performed using an aerosol nebulization system assembled at the Center for Heath and the Environment at the University of California Davis (Fig. 1). AgNP suspensions were aerosolized into fine droplets using a BGI 6-jet collision nebulizer (Waltham, Massachusetts). Compressed air for the nebulizer was generated using an oil-free compressor (California Air Tools, San Diego, California), dehumidified using compressed air dyers (Wilkerson, Richland, Michigan), and filtered with a Motor Gard M-610 filter (Motor Gard, Manteca, California). Nebulizer inlet pressure was 20 psi. Output from the nebulizer was passed through a custom fabricated heater, then directed through 2 diffusion dryers (TSI, Shoreview, Minnesota) to remove water from the particles. Particles were then routed through a custom built charge neutralizer equipped with a Krypton-85 source before entering a 72-port nose-only exposure chamber (Raabe *et al.*, 1973). Components were connected using steel pipe. Rats were housed in nose-only exposure tubes (Teague Enterprises, Woodland, California) for duration of the exposure. Excess AgNPs were drawn from the chamber and through a second Motor Gard filter by a high volume vacuum pump (Gast, Benton Harbor, Michigan). The exposure chamber was maintained at 0.5–1.0 in. water pressure below room pressure. A peristaltic pump (Cole-Parmer, Vernon Hills, Illinois) was used to supply the nebulizer with suspended AgNPs which were maintained at a constant level. A flask held the stock suspension which was constantly stirred and kept on ice to reduce aggregation of particles.

*Exposure characterization*. The temperature and humidity of the room and exposure atmosphere were monitored for the duration of the exposure. For each 6 h exposure, the following samples were taken, distributed throughout the exposure: 6 mass concentration samples, 4 x-ray fluorescence (XRF) samples, 2 cascade impactor samples, 2 transmission electron microscopy (TEM) samples, and real-time size mobility particle scanner (SMPS) measurements. A SMPS (TSI 3071 classifier and 3010 condensation particle counter) was used to measure the number of particles from 12 to 600 nm. Samples were logged at 15-min intervals. Total mass concentration of AgNPs was determined by gravimetric measurement of 25 mm Pallflex membrane filters (Pall Life Sciences, Port Washington, New York) with samples collected at 1 l/min for 15 min. XRF samples were collected on 25 mm Pall Teflo filters (Pall Life Sciences) at 3 l/min for 5 min and the mass of Ag on the filters was determined by Chester Labnet (Tigard, Oregon). An 8-stage Mercer-style cascade impactor (Raabe, 1979) was employed to measure larger particle agglomerates collected on 25 mm Pallflex membrane filters at 1 l/min for 30 min. Aerosolized AgNPs for TEM were collected onto a formvar carbon film supported on a 400-mesh copper grid (3 mm in diameter) (Ted Pella, Reading, California) at room temperature using an electrostatic precipitator. TEM images were acquired using a Phillips CM-12 TEM operating at 120 kV. Particle size was confirmed using dynamic light scattering (DLS)

Downloaded from http://toxsci.oxfordjournals.org/ at Government on August 9, 2016

**TABLE 1.** *in vivo* Aerosol Studies of Silver Nanoparticles that Quantified Silver Concentration in the Lung

| Reference | Physical Properties | Exposure Regimen | Dose | Species | PE Timepoint | Endpoints | Findings | Measured Ag in Lung (Method) |
|---|---|---|---|---|---|---|---|---|
| Ji *et al.* (2007) | 18 nm uncoated generated in ceramic heater | 6 h/day<br>5 day/week<br>For 4 week whole body | 0.5, 3.5, and 61 $\mu g/m^3$ | Rat (S/D) Male and female | 0 h | Hematology<br>Organ Wt<br>Histopathology<br>Silver Quantification | No significant effects | Low Male Female<br>Mid 0.32 0.27 ng/g<br>Hi 1.25 1.19 ng/g<br>(AA) 1.18 1.50 $\mu g/g$ (ww) |
| Sung *et al.* (2009) | 18 nm uncoated generated in ceramic heater | 6 h/day<br>5 day/week<br>For 13 week whole body | 49, 133, and 515 $\mu g/m^3$ | Rat (S/D) Male and female | 0 h | Hematology<br>Organ Wt<br>Histopathology<br>Silver Quantification | No change in organ weights. Alveolar inflammation and macrophage accumulation in high dose animals | Low Male Female<br>Mid 0.30 0.61 $\mu g/g$<br>Hi 4.24 5.45 $\mu g/g$ 14.7 $\mu g/g$<br>(AA) 20.6 (ww) |
| Stebounova *et al.* (2011) | 5 nm uncoated, suspended in water | 6 h/day<br>5 day/week<br>For 2 week whole body | 3.3 $mg/m^3$ | Mouse (C57BL/6) male | 0 h and 3 weeks | BAL Silver Quantification | Increase in BAL macrophages and neutrophils at both timepoints.<br>No increase in LDH<br>Increase in IL-12 and KC at 0 h. | 31 $\mu g/g$ (0 h)<br>10 $\mu g/g$ (3 weeks)<br>(ICP-AES) (dw) |
| Takenaka *et al.* (2001) | 15 nm uncoated Spark generated | Single 6 h whole body | 133 $\mu g/m^3$ | Rat (Fischer 344) | 0 h, 1, 4, and 7 days | Silver Quantification | Decrease in concentration of Ag in lung over time post-exposure. | 2.38 $\mu g/g$ (0 h)<br>0.90 $\mu g/g$ (1 day)<br>0.20 $\mu g/g$ (4 days)<br>0.10 $\mu g/g$ (7 days)<br>(ICP-MS) (ww) |
| Kwon *et al.* (2012) | 20 nm uncoated generated in ceramic heater | Single 6 h Nose-only | 2.9 $mg/m^3$ | Mouse (C57BL/6) Male | 0 and 24 h | BAL<br>Western blot<br>Silver Quantification | No change in BAL protein or LDH levels and no change in BAL cells Increase in ERK1/2 and p38 at 0 h and JNK at 0 and 24 h | 0.51 $\mu g/g$ (0 h)<br>0.12 $\mu g/g$ (24 h)<br>(AA) (dw) |
| Braakhuis *et al.* (2014) | 15 nm (spark generated) and 410 nm (PVP-coated 200 nm primary particles) | 6 h/day for 4 days Nose-only | 179 $\mu g/m^3$ (15 nm) 167 $\mu g/m^3$ (410 nm) | Rat (Fischer 344) | 1 and 7 days | BAL<br>ELISA<br>TEM<br>Histopathology<br>Silver Quantification | Neutrophil influx (15 nm)<br>Increase in proinflammatory cytokines | 15 nm:<br>3.4 $\mu g/g$ (24 h)<br>1.3 $\mu g/g$ (7 days)<br>410 nm:<br>6.0 $\mu g/g$ (24 h)<br>3.9 $\mu g/g$ (7 days)<br>(HP-ICP-MS) |

Abbreviations: S/D, Sprague Dawley; BAL, bronchoalveolar lavage fluid; PE, post-exposure; AA, atomic absorption spectroscopy; ICP-AES, inductively coupled plasma atomic emission spectroscopy; HP-ICP-MS, high-performance inductively coupled plasma mass spectroscopy; ww, wet organ weight; dw, dry organ weight.

Downloaded from http://toxsci.oxfordjournals.org/ at Government on August 9, 2016

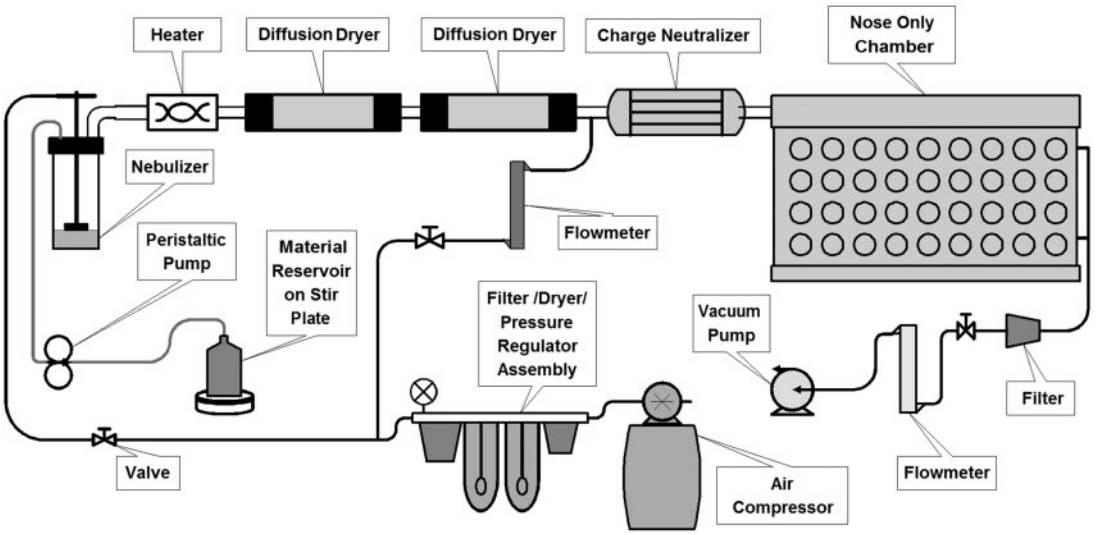


FIG. 1. Silver nanoparticle aerosol generation and exposure system. Particles in suspension are aerosolized into water droplets using a 6-jet collison nebulizer. Water is removed using diffusion dryers and particle charge is neutralized using a krypton-85 beta emission source. Dry particles are directed to a nose-only exposure chamber.

TABLE 2. AgNPs Characterization Data

| Measurement | Citrate Buffer | 20 nm AgNP | 110 nm AgNP |
|---|---|---|---|
| Mass concentration metals (XRF) ($mg/m^3$) | NA | $7.2 \pm 0.8$ | $5.3 \pm 1.0$ |
| Mass concentration—gravimetric ($mg/m^3$) | $5.0 \pm 1.7$ | $13.9 \pm 2.3$ | $12.4 \pm 2.5$ |
| SMPS size (nm) (geometric mean, geometric SD) | 76.6 $\sigma$ 1.8 | 77.4 $\sigma$ 1.8 | 78.2 $\sigma$ 1.8 |
| SMPS particle number (12.6–593 nm)(number of particles/$cm^3$) | $1.8 \times 10^6 \pm 0.2 \times 10^6$ | $2.2 \times 10^6 \pm 0.4 \times 10^6$ | $1.3 \times 10^6 \pm 0.3 \times 10^6$ |
| DLS hydrodynamic size (nm) (Z-average ± dispersity) | NA | $27.06 \pm 0.15^a$<br>$27.24 \pm 0.21^b$ | $111.2 \pm 0.2^a$<br>$106.6 \pm 0.2^b$ |

Notes: All values are mean ± standard deviation unless otherwise noted.
[a]Particles from sealed container.
[b]Particles recovered from nebulizer at end of exposure.

on AgNPs from sealed containers and on excess material from the nebulizer at the end of exposure to monitor integrity of the particles and uniformity during the nebulization. DLS was performed on samples diluted 1:100 in milliQ water with a Zetasizer Nanosizer ZEN1690 (Malvern Instruments, UK) equipped with a He-Ne 633 nm laser. Diluted sample absorbance was determined using a PharmaSpec UV-1700 spectrophotometer (Shimadzu, Santa Clara, California) and the refractive index of silver was obtained from the NIST database (Smith and Fickett, 1995). Stability of nanoparticles over the duration of the experiment was confirmed by tests on suspended particles before and after use in the nebulizer as well as the tests described above for the atmosphere. Results are given in Z-average diameter (nm) in Table 2.

*Animals*. Twelve-week-old male adult Sprague Dawley rats were obtained from Harlan Laboratories and acclimated for 1 week prior to exposure. Rats were housed 2 per cage and provided Laboratory Rodent Diet (Purina Mills, St Louis, Missouri) and water *ad libitum*. All animal experiments were performed under protocols approved by the University of California Davis IACUC in accordance with National Institutes of Health guidelines. Rats were conditioned to the exposure tubes in the week prior to exposure by being housed in tubes for progressively longer periods of time.

Animals used for silver staining and bronchoalveolar lavage were dosed nose only to either aerosolized 20 nm AgNP, 110 nm AgNP, or citrate buffer for 6 h. Animals were euthanized at 1, 7, 21, and 56 days post-exposure using Beuthanasia-D at 7.5 ml/kg and exsanguination. The abdominal and thoracic cavities were opened, the trachea cannulated, and the left lung lobe isolated by clamping the left primary bronchus. The right lung lobes were lavaged using 8 ml of 0.9% sterile saline in a 12-ml syringe, washing with the same aliquot 3 times. The resultant bronchoalveolar lavage fluid (BALF) was collected into 15 ml round bottom tubes and kept on ice until processed. The right primary bronchus is then tied off, the right lobes were removed, and the left lobe with the trachea was perfused with 4% paraformaldehyde at 30 cm of water pressure for 1 h.

A second set of animals was used for dosimetry and clearance, exposed as described above, and euthanized at the end of the exposure ($T_0$) or at 1, 7, 21, and 56 days post-exposure. The lungs and extrapulmonary airways were removed en bloc with the trachea cut just below the larynx. Lobes were removed at the lobar bronchus and each lobe and the remaining trachea and bronchi were placed in 15 ml conical tubes and flash frozen in liquid nitrogen. Samples were stored at −80°C until processed for ICP-MS measurement of silver content.

Downloaded from http://toxsci.oxfordjournals.org/ at Government on August 9, 2016

*Silver staining*. Two 1-mm blocks representing short and long axial path airways of the 4% paraformaldehyde fixed left lobe were embedded in paraffin and sectioned onto poly-L-lysine-coated slides. Silver was visualized using a variation of a published method for autometallography (Danscher and Stoltenberg, 2006; Hacker *et al*., 1988). A silver enhancement kit for light and electron microscopy (Ted Pella Inc, Redding, California) was used (Wang *et al*., 2014) and all slides were developed under identical conditions to facilitate comparisons across groups and timepoints. Paraffin-embedded samples were deparaffinized rehydrated and stained with equal volumes of enhancer and developer for 15 min. Cytospin slides were hydrated in PBS, stained for silver as described above, and then lightly counter stained with diluted 1:1000 methylene blue azure II stain. Slides were imaged using an Olympus BH-2 light microscope.

*BALF macrophages*. BALF was centrifuged at 2000 rpm and 4°C for 10 min to pellet cells. BALF supernatant was removed and stored for a different study. The cell pellet was resuspended in 2 ml sterile 0.9% saline and the total number of cells and non-viable cells, using Trypan blue assay, were counted. A cytospin slide was prepared from the resuspended BALF cells for silver staining and quantitation of macrophages as a percentage of the total cells. The percentage of silver-positive BALF macrophages was determined by counting silver-stained cytospins for silver positive and negative macrophages on autometallography-stained cytospin slides at ×40 magnification. A total of 500 cells were counted per slide. To further assess the silver load in the macrophage population, a semi-quantitative scoring system was employed. Silver-positive macrophages were subdivided into light, moderate, and heavy staining for silver as shown in Supplementary Figure 1. A total of 200 silver positive macrophages were scored per animal; all silver positive macrophages were scored if less than 200 were silver positive. The fractions of macrophages with light, moderate, and heavy silver content macrophages were used to determine a score for each animal using the formula:

$$S = ((M_T \times f_L) + (M_T \times f_M \times 2) + (M_T \times f_H \times 3))/1000,$$

where $S$ is the silver score, $M_T$is the total recovered macrophages ($\times 10^4$) per ml of BALF, and $f_L$, $f_M$, and $f_H$are the fractions of silver positive macrophages in the macrophage population (Anderson *et al*., 2014).

*Spectral profiling and enhanced dark field imaging*. AgNPs deposition was qualitatively evaluated in unstained paraffin embedded lung sections using a Cytoviva-enhanced dark field microscope (Cytoviva, Auburn, Alabama). Lung sections were evaluated for qualitative assessment of AgNP deposition at 1, 7, and 21 days following exposure at a magnification of × 100. Spectral analysis of AgNPs was performed utilizing hyperspectral dark field microscopy (Cytoviva). To generate a mean spectral profile of 20 and 110 nm AgNPs, particles were loaded onto premium clean microscope slides and mean spectrums were created utilizing pixels with an intensity greater than 1000. To determine changes in AgNP spectrums following macrophage internalization unstained paraffin embedded tissue samples were assessed by hyperspectral dark field microscopy. AgNPs within cells were assessed by focusing on the nucleus of the cell and a hyperspectral image was collected at a magnification of × 100. To generate spectral profiles a minimum of 1000 pixels of AgNPs were collected to form a region of interest that was used to create a mean spectrum. This spectrum was then normalized and compared with the normalized original spectrum of the corresponding AgNP. Finally, to understand intercellular modifications in AgNP spectra, AgNPs were incubated for 24 h in artificial phagolysosomal fluid with a pH of 4.5. AgNPs were then centrifuged for 10 min at 14 000 rpm (20 817 g) and resuspended in water before being loaded onto premium clean microscope slides for assessment by hyperspectral dark field microscopy.

*TEM of BALF macrophages*. Cells recovered from BALF were fixed with Karnovsky's fixative (0.9% glutaraldehyde/0.7% paraformaldehyde in cacodylate buffer, adjusted to pH 7.4, 330 mOsmol/kg $H_2O$) and suspended in agar blocks. Blocks were embedded in Araldite 502 resin and osmicated (Van Winkle *et al*., 1995). Sections were cut using a Leica Ultracut UCT ultramicratome and Diatome diamond knives. TEM images of BALF macrophages were obtained using a Philips CM120 electron microscope.

*Silver deposition quantification*. Concentration of silver in the extrapulmonary airways and lung lobes was determined using ICP-MS. Tissues were lyophilized using a Labconco FreeZone 2.5 (Kansas City, Missouri) freeze drying system and weighed to determine tissue dry weight. Tissue was digested with 70% trace metal grade nitric acid (Fisher) and heated to 70°C for 2 h. Samples were cooled to room temperature, an equal volume of 30% $H_2O_2$ was added. Samples were reheated to 70°C for 12 h to break down remaining lipids and finally cooled to room temperature and diluted 5:1 with milliQ water for analysis by the UC Davis/Interdisciplinary Center for Plasma Mass Spectrometry using an Agilent 7500CE ICP-MS (Agilent Technologies, Palo Alto, California). The samples were introduced using a MicroMist Nebulizer (Glass Expansion, Pocasset, Massachusetts) into a temperature controlled spray chamber with Helium as the collision cell gas. Instrument standards were diluted from Certiprep Ag Standard (SPEX CertiPrep, Metuchen, New Jersey) to 0.5, 1, 10, 50, 100, 200, and 500 ppb in 3% Trace Element $HNO_3$ (Fisher Scientific) in 18.2 Mohm-cm water. A NIST 1643E Standard (National Institute of Standards and Technology, Gaithersburg, Maryland) was analyzed initially and QC standards consisting of a Certiprep Ag Standard at a concentration of 100 ppb was analyzed every 12th sample as a quality control. Sc, Y, and Bi Certiprep standards (SPEX CertiPrep) were diluted to 100 ppb in 3% $HNO_3$ and introduced by peripump as an internal standard.

*Deposition modeling*. Estimation of deposited dose of AgNPs was performed using the Multi-Path Particle Dosimetry Model (MPPD) v2.1 software (Applied Research Associates, Albuquerque, New Mexico). Input parameters are listed in Table 3.

*Statistics*. Data are reported as mean ± standard error of the mean unless otherwise stated. Statistical outliers were eliminated using the extreme deviate method (Graphpad, La Jolla, California). Multivariate analysis of variance (MANOVA) was applied against particle size, surface coating, time-point, and dose when appropriate. Multiple comparisons for factors containing more than 2 levels were performed using Fisher's protected least significant difference (PLSD) method. Pair-wise comparisons were performed individually using a 1-way ANOVA followed by PLSD post hoc analysis. *P*-values of less than 0.05 were considered statistically significant.

Downloaded from http://toxsci.oxfordjournals.org/ at Government on August 9, 2016

Non-parametric analysis of macrophage scoring data were performed using the Kruskal-Wallis ANOVA to assess differences by timepoint and the Mann-Whitney test to compare between particle types. Statistics was performed using STATISTICA 64 (Tulsa, Oklahoma).

## RESULTS

### *Exposure Characterization*

All AgNPs were supplied by the NCNHIR and National Characterization Laboratory (NCL). Use and characterization of these particles for bolus intratracheal instillation and oropharyngeal aspiration in rats and mice, respectively, have been reported previously (Anderson *et al.*, 2014; Wang *et al.*, 2014). Briefly, NCL characterization of AgNPs from suspension using TEM and the DLS found that measurements were in agreement with the primary particle size reported by the manufacture. Additionally, endotoxin levels were below level of detection for both particle sizes. Rats were exposed nose only for 6 h to an atmosphere of nebulized citrate buffer (controls) or citrate-coated AgNPs with a primary size of either 20 or 110 nm mean diameter. A schematic diagram of the aerosol exposure system is presented in Figure 1. The BGI 6-jet Collison nebulizer was chosen for its ability to generate the concentration and air flow rate sufficient for the rat nose-only exposure chamber (Schmoll *et al.*, 2009) and because the fluid jar can be refilled during operation without changing the exposure output. The nebulizer was operated at 20 psi (6.9 kPa) for a manufacturer-specified output of 12 l/min, confirmed with a flow meter. Chamber temperature was 19–23°C; chamber humidity was 30%–50%.

The atmosphere was characterized (Table 2 and Figs. 2 and 3) and all measured values are averaged from 3 exposures for each of the AgNPs and 2 exposures for citrate buffer. The total particle mass concentration determined gravimetrically was $5.0 \pm 1.7\ mg/m^3$ for citrate buffer, $13.9 \pm 2.3\ mg/m^3$ for 20 nm AgNP, and $12.4 \pm 2.5\ mg/m^3$ for the 110 nm AgNP. The airborne concentration of silver using XRF analysis was $7.2 \pm 0.8\ mg/m^3$ and $5.3 \pm 1.0\ mg/m^3$ for 20 and 110 nm AgNPs, respectively (Table 2 and Fig. 2A). The differences in mass concentration between the gravimetric and XRF measurements can be attributed to the 2mM citrate buffer used to stabilize and coat the AgNPs in suspension. Because the mass of AgNPs determined using a gravimetric method is inflated by the citrate salts, dose calculations are based on the mass concentration measured by XRF.

TEM of both AgNPs from the aerosol system (Figs. 2B and 2C) indicated expected sizes based on the measurements of particles from the suspension. Scanning mobility particle sizer (SMPS) data are presented in Table 2 and Figure 3. Particle number concentration shows that the citrate buffer exposure is similar to the 20 nm AgNP data in both size and number as measured by SMPS (Table 2). The 110 nm AgNP have a bimodal profile with a peak at 78.2 nm and a secondary peak at 120 nm (Fig. 3D). Cascade impactor data show that 65% of 20 nm AgNP and 61% of 110 nm AgNP were present as particles less than 1.1 μm in size (Figs. 3B and 3E). If the next stage is included, particles up to 1.6 μm, the fractional percentages increase to 82% and 81% for 20 and 110 nm AgNPs, respectively, indicating that most of the particles generated were less than 1.6 μm.

To assess any change in particle size during the exposure, DLS was performed on AgNPs both before use from sealed containers (new) and from suspension collected from the nebulizer at the end of the exposure (recovered) (Table 2 and Figs. 3C and 3F). The hydrodynamic diameter for the 20 nm AgNP was 27.0 (± 1.0) nm for new particles (circles) and 27.2 (± 1.0) for recovered particles (diamonds), while that of the 110 nm AgNP was 111.2 ± 0.2 nm for new (circles) and 106.6 ± 0.2 nm for recovered particles (diamonds). These findings indicate maintenance of particle integrity within the nebulizer. The small peak at 5.5 μm for the 20 nm AgNP suggests a small amount of aggregation.

**TABLE 3.** Multi-Path Particle Dosimetry (MPPD) Model Input Parameters and Results

| Input Parameters | 20 nm | 110 nm |
|---|---|---|
| Species | Rat | Rat |
| FRC volume (ml)[a] | 4.0 | 4.0 |
| Head volume (ml)[a] | 0.42 | 0.42 |
| Density | 7.24 | 7.24 |
| Diameter (CMD) (nm) | 77[b] | 110[c] |
| Geometric SD ($\sigma_g$) | 1.8 | 1.8 |
| Concentration ($mg/m^b$) | 7.2 | 5.3 |
| Breathing frequency[a] ($min^{-1}$) | 102 | 102 |
| Tidal volume[a] (ml) | 2.1 | 2.1 |
| Inspiratory fraction[a] | 0.5 | 0.5 |
| Pause fraction[a] | 0 | 0 |
| Breathing scenario | Nasal | Nasal |
| Clearance rate[d] ($day^{-1}$) | 0.00515 | 0.00515 |
| Output results | | |
| Deposition fraction alveolar region | 0.124 | 0.100 |
| Deposition fraction conducting airways | 0.031 | 0.029 |
| Thoracic deposited fraction | 0.155 | 0.129 |
| Retained alveolar fraction at 56 days | 0.348 | 0.317 |

[a]Default value from program (http://www.ara.com/products/mppd.htm).
[b]SMPS geometric mean diameter.
[c]SMPS secondary peak diameter.
[d]Ji and Yu (2012) *Toxicology Research*.

*Macrophage clearance of AgNPs*. There was no significant difference in the total number of BALF recovered macrophages in control animals irrespective of the timepoints. Macrophages, as determined by autometallography and analysis of cell morphology, were the predominant silver containing cells (Supplementary Fig. 1). The number of non-viable cells ranged from 2.1% to 3.8% for citrate-exposed (control) rats and 1.7% to 4.5% for AgNPs-exposed groups. At no timepoint were AgNPs-exposed rats significantly different than citrate-exposed controls in the percent of non-viable cells recovered in BALF. There was a significant decrease in the number of macrophages in the BALF for both particle types at 1 day post-exposure; animals exposed to 20 and 110 nm AgNPs had 40% and 50% less macrophages (Fig. 4A). At 7 days post-exposure, the 20 nm AgNP produced significantly elevated numbers of BALF macrophages when compared with either the same day controls or the 20 nm AgNP at 1 day post-exposure. However, the 110 nm AgNP group did not produce a significant change at 7 days post-exposure compared with controls. By 21 and 56 days post-exposure, there were no significant differences in recovered BALF macrophages between the 3 exposure groups or between the 21 and 56 day timepoints. Finally, both 20 and 110 nm AgNPs produced significantly more BALF macrophages at 21 and 56 days post-exposure than their respective 1 day levels.

As expected, there were no silver positive macrophages in citrate buffer-only exposed rats. The highest percentage of silver positive macrophages was observed at 1 day post-exposure with 20 nm AgNP-exposed rats having 64% silver positive

Downloaded from http://toxsci.oxfordjournals.org/ at Government on August 9, 2016

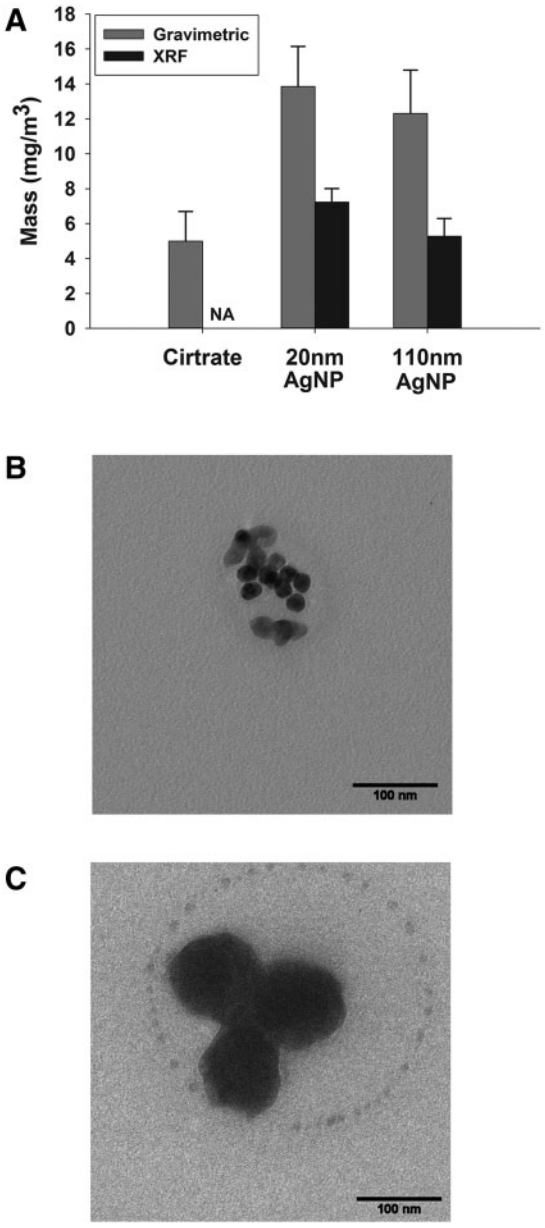


FIG. 2. Aerosol AgNPs concentration and morphology of aerosolized particles. Mass concentration comparison of exposure to citrate buffer, 20 or 110 nm AgNP (A) determined by gravimetric filter (gray bars) and XRF filter analysis (black bars). Transmission electron micrographs (TEM) of 20 (B) and 110 nm AgNP (C). Bar = 100 nm.

staining macrophages and those exposed to 110 nm AgNP having a significantly lower percentage (52%) of positive staining macrophages (Fig. 4B). At 7 days post-exposure, animals exposed to both 20 and 110 nm AgNPs had a significantly less silver positive macrophages (22% and 19%, respectively) versus 1 day post-exposure. Between post-exposure days 7 and 21 or 56, the percentage of silver positive macrophages did not change significantly in animals given 20 nm AgNPs. However, rats exposed to 110 nm AgNP at 21 days had only 5% silver positive macrophages, which was significantly less than in the 20 nm AgNP-exposed group at the same day and the 110 nm AgNP-exposed group at 7 days. This downward trend continued at 56 days post-exposure when only 1.5% of macrophages recovered from the 110 nm AgNP-exposed rats were silver positive.

To further examine the silver burden in the macrophage population, a weighted scoring system was used to categorize macrophages as light, moderate, or heavy for silver staining (Fig. 4C). This system took into account both the relative fraction of each level of staining and the total number of recovered silver positive macrophages per milliliter of BALF recovered. Animals exposed to the 110 nm AgNP scored significantly lower than the 20 nm AgNP at all timepoints. While having fewer silver positive macrophages accounts for this difference at the 21 and 56 day post-exposure timepoints, this does not explain findings at the earlier (1 and 7 days) timepoints. As stated above, at 1 day post-exposure, the animals exposed to 20 and 110 nm AgNPs had 64% and 52% silver positive macrophages, respectively. This was a small but significant difference. However, the silver macrophage scores for the 1 day timepoint were 6.0 and 3.3 for the 20 and 110 nm AgNP-exposed groups, respectively, a difference of 45%, suggesting that macrophages recovered from animals exposed to 20 nm AgNP were more particle laden. The differences in macrophage silver burden scores between the particle sizes at 7 days post-exposure are influenced by the difference in total recovered macrophages noted previously. The 110 nm AgNP-exposed animals had significant decreases in silver score at all timepoints after 1 day post-exposure, with a 96% decrease in score from 1 day to 56 days post-exposure. In contrast, rats exposed to 20 nm AgNP had a significant decrease (69%) only between the 1 day and 56 days post-exposure timepoints; the differences between 1 day and 7 days, and 1 day and 21 days had low $P$-values of $P = 0.096$ and $P = 0.068$, respectively.

*Silver in lung tissue.* The abundance and distribution of silver were determined in lung tissue using ICP-MS on lung lobes and extrapulmonary airways and autometallography on tissue sections from the left lung lobe, respectively. Citrate buffer-exposed animals did not have detectable silver using either ICP-MS or autometallography. The spatial distribution of silver at the end of 6 h exposures ($T_0$) did not vary between the 2 AgNPs sizes (Supplementary Fig. 2). Following aerosol exposure, silver measured by ICP-MS in the right middle lobe tissue was 1.66 and 1.57 μg/g for the 20 and 110 nm AgNP, respectively (μg silver/g tissue). The total mass of silver in the thoracic respiratory system at $T_0$ was calculated by summing the measured mass of silver in each lobe, the trachea, and the lobar bronchus (Supplementary Fig. 2). The total mass of silver was 321 and 357 ng for the 20 and 110 nm AgNPs, respectively. At 1 day post-exposure, the 20 nm AgNP-exposed group had significantly less silver than the animals examined at the end of exposure ($T_0$) (Fig. 5). By 7 days post-exposure, retained silver was significantly less than at $T_0$ and at 1 day post-exposure for animals exposure to 20 or 110 nm AgNPs. Interestingly, there appeared to be a downward trend in retained silver levels at the 21 and 56 day post-exposure timepoints, but there were no significant reductions when compared with 7-day timepoint. There was no observed difference in tissue clearance between the 2 particles sizes.

The distribution of the silver in the tissue was investigated using autometallography. There was no silver positive staining in proximal airways at any timepoint (data not shown). The pattern of silver staining in the alveolar duct junction region was similar for the 2 sizes of AgNPs (Figs. 6 and 7). At 1 day post-exposure, the pattern of silver staining consisted primarily of macrophages (arrows, Figs. 6A and 6B and 7A and 7B) with occasional staining along the epithelium (open arrows). At 7 days post-exposure, silver positive macrophages were present, and

Downloaded from http://toxsci.oxfordjournals.org/ at Government on August 9, 2016

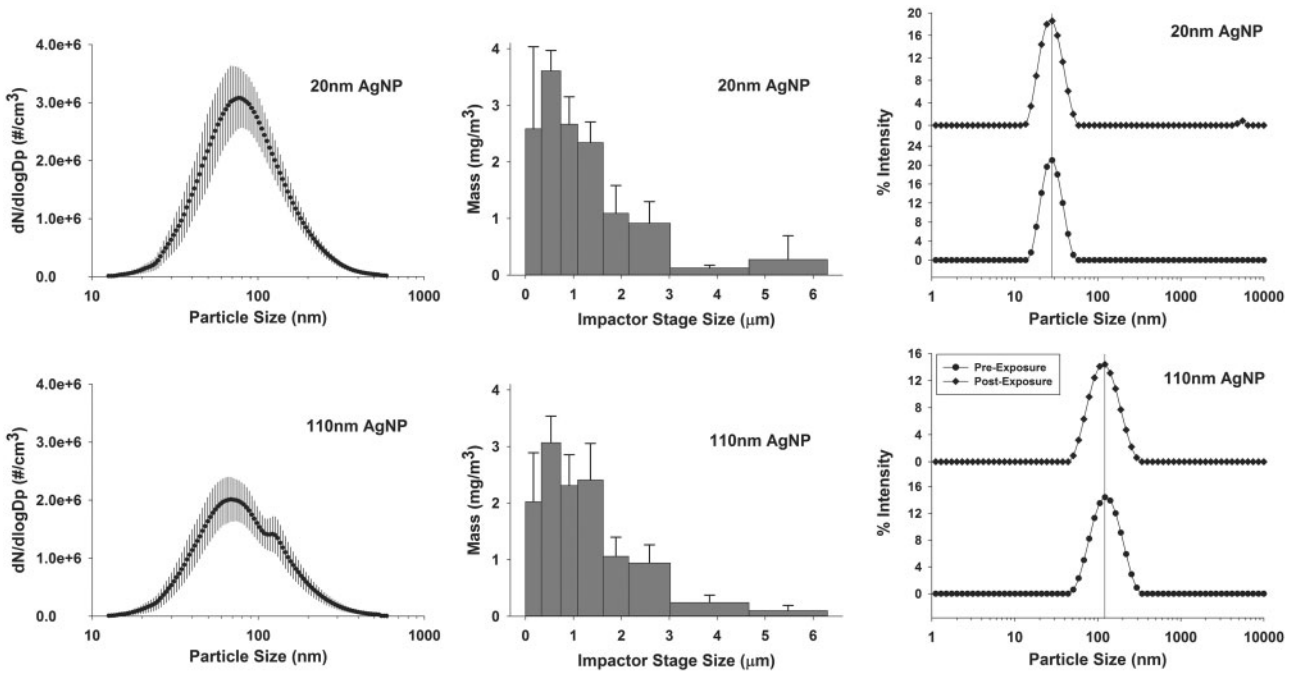


FIG. 3. Aerosol AgNPs characterization. Characterization of AgNPs aerosol was performed using a scanning mobility particle sizer (A, D), cascade impactor (B, E), and dynamic light scattering (DLS) (C, F). SMPS peak particle number at 77.4 nm for 20 nm AgNP and (E) 78.2 nm for 110 nm AgNP. Note the shoulder in the 110 nm AgNP trace at 120 nm (D). Mass concentration of size fractions was determined using a Merced type cascade impactor type (B, E). This indicates that there were some agglomerates of particles in the sample. Particle size in suspension was determined by DLS (C, F). Samples from manufacturer sealed containers (circles) and particles recovered from nebulizer at the end of exposure (diamonds) are very similar indicating lack of degradation. SMPS data are geometric mean $\pm \sigma_g$ (geometric standard deviation), cascade impactor data are mean ± SD, and DLS is Z-average diameter.

there was staining of the basement membrane in the terminal bronchiole/alveolar duct junction region (arrow heads, Figs. 6 and 7). The staining of the basement membrane was most intense for both AgNPs at 21 days and reduced, but still present at 56 days.

### *Localization of AgNPs with enhanced dark field imaging and hyperspectral profiling*

Assessment of unstained paraffin-embedded lung sections by enhanced dark field microscopy demonstrated cellular uptake of 20 (Figs. 8A–C and 8G) and 110 nm AgNPs (Figs. 8D, 8E, and 8F). Primarily AgNPs were found to be internalized by alveolar macrophages and epithelial cells (Figs. 8A, 8D, and 8G). Intracellular modifications of AgNPs in lung macrophages were evaluated by hyperspectral analysis and compared with the spectral profiles of 20 (Fig. 8H, black line) and 110 nm (Fig. 8I, black line) AgNPs suspended in water or artificial lysosomal fluid (ALF). Following macrophage internalization the spectral profiles of 20 and 110 nm AgNPs were found to undergo a red shift (Figs. 8H and 8I, red lines) possibly due to addition of intracellular proteins following internalization. Nanoparticles are often concentrated in phagolysosomal compartments following macrophage internalization. To further characterize these intracellular modifications in AgNP spectra, 20 and 110 nm AgNPs were incubated for 24 h in ALF and assessed for changes in mean spectral profiles. The mean spectrum of 20 nm AgNP following incubation in ALF was found to undergo a red shift that matches the spectral profile of 20 nm AgNP following macrophage internalization (Fig. 8H, blue). Incubation in ALF was found to also cause a red shift in the 110 nm AgNP spectrum producing a profile similar to 110 nm AgNP within the macrophages (Fig. 8I, blue).

*Macrophage TEM.* TEM micrographs of recovered macrophages from BALF show small silver particles (Fig. 9). These small particles, which may be regenerated *in situ* (Glover *et al.*, 2011; Levard *et al.*, 2012; Marchiol *et al.*, 2014), originate from both 20 (Figs. 9A–D) and 110 nm AgNPs (Fig. 9E). A large number of these small particles can be seen forming an approximately 100 nm sphere (Figs. 9A and 9B). Also observed were less organized groupings of these small particles in clumps (Figs. 9C and 9D) and in chains (Fig. 9E).

*Calculation of dose.* An estimate of the deposited dose of silver was made using the MPPD v2.11 software (http://www.ara.com/products/mppd_download.htm). Animal parameters used were from Ji *et al.* (2007; Ji and Yu, 2012). Particle parameters were based on characterization of data collected during exposures (Table 3). Particle density of 7.24 g/cm$^3$ was used in the model. This figure was calculated based on the mass fraction contributed by the AgNPs and citrate buffer to particle mass. AgNPs and trisodium-citrate made up 63% and 37% of particle mass, respectively, assuming most water was removed from the particles before inhalation. Changing particle density in the model resulted in very small changes in deposition fractions. Deposition of particles less than 150 nm is caused primarily from diffusion forces where particle density is not a factor and this was expected (Londahl *et al.*, 2014). The deposition fraction from the MPPD model was used to calculate thoracic deposition using the formula:

$\text{Dose} = \text{Df} * \text{C} * \text{MV} * \text{t}$, where Df is the deposition fraction, C is the particle concentration in exposure chamber, MV is the respiration minute volume, and t is the exposure duration in minutes. The MPPD model produced a Df of 0.155 and 0.129 for the 20 and 110 nm AgNPs, respectively (Table 3). With the

Downloaded from http://toxsci.oxfordjournals.org/ at Government on August 9, 2016

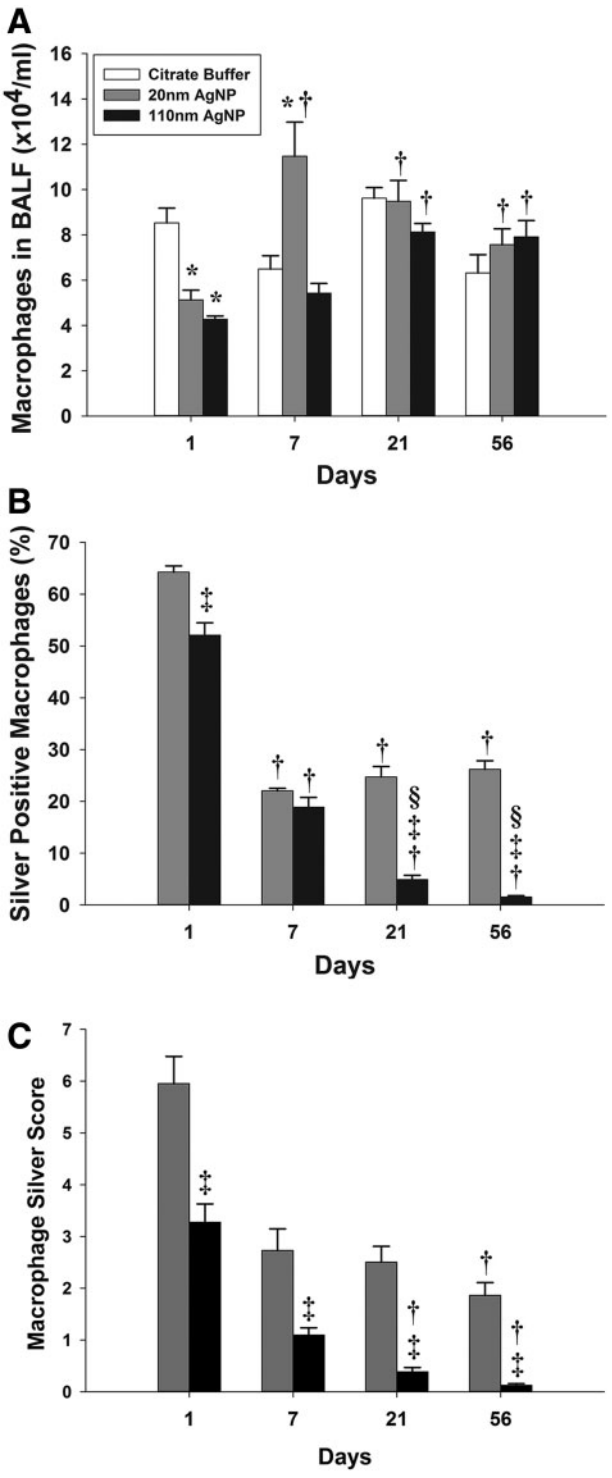


FIG. 4. Total and silver positive macrophages recovered from bronchoalveolar lung lavage at 1, 7, 21, and 56 days following exposure. Number of macrophages recovered from BALF (A). Percent of silver positive macrophages that are positive for silver staining based on autometallography and light microscopy at × 40 magnification (B). Macrophages were scored depending on the intensity of silver staining as light, moderate, and heavy as shown in Supplementary Figure 1 (C). Compared with the 20 nm 1 day score, the 20 nm 7 day had a $P = 0.096$ and the 20 nm 21 day was $P = 0.068$. Asterisk (*), significantly different than citrate buffer at same timepoint; dagger (†), significantly different than 1 day timepoint for same particle type; double dagger (‡), significantly different than 20 nm AgNP at same timepoint; and delta (§), significantly different than 7 day timepoint for same particle type ($P < 0.05$) ($n = 6$).

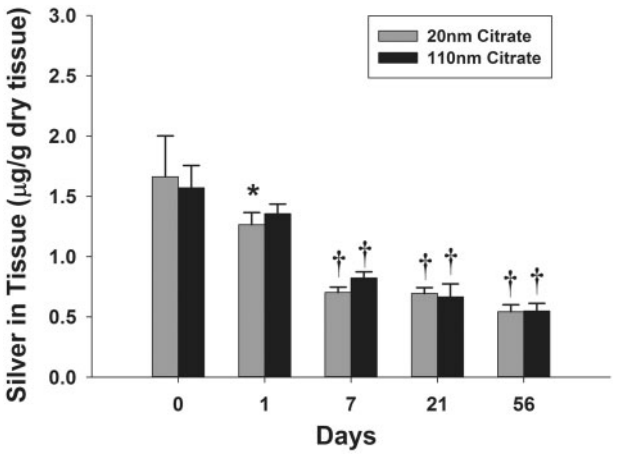


FIG. 5. Silver quantification using ICP-MS in the lung tissue following exposure. The amount of silver retained in the right middle lobe at 1, 7, 21, and 56 days post-exposure (C). Asterisk (*), significantly less than $T_0$ time-point for same particle type ($P < 0.05$); dagger (†), significantly less than $T_0$ and $T_1$ time-point for same particle type ($P < 0.05$) ($n = 6$).

exposure concentration of 7.2 and 5.3 mg/m$^3$ (for 20 and 110 nm AgNPs, respectively) and a 360-min exposure, the deposited dose of silver in the lungs and trachealbronchial airways would be 80 μg for the 20 nm AgNP and 59 μg for the 110 nm AgNP. The bulk of the deposition is predicted to be in the alveolar region (Table 3). The MPPD model was also used to predict clearance. The model predicts that 34.8% and 31.7% of 20 and 110 nm particles deposited in the lung, respectively, would be retained after 56 days.

## DISCUSSION

We tested the effect of particle size on AgNP deposition and retention in the rat lung following inhalation exposure. We found that smaller particles (20 nm) are cleared less readily than larger particles (110 nm), showing an increase in persistence in the lung when a similar mass of particles is delivered by an aerosol. This slower removal of the smaller particles may be related to the higher particle number of 20 nm AgNP delivered in the aerosol than larger size particles for the same mass concentration. Calculation of the difference in number of particles given the same mass of particles yields a ratio of 166:1 when comparing 20 to 110 nm particles. Macrophages continue to be involved in particle clearance, especially of the smaller particles, even 56 days after exposure. Autometallography staining for silver indicates accumulation of silver in the terminal bronchiole alveolar duct junction, prominently colocalized with the subepithelial extracellular matrix 21 days after exposure. This may indicate preferential binding or sequestration of the AgNPs or silver ions at this site. Remarkably, when the entire lung was analyzed for silver content using ICP-MS, approximately one-third of the initial silver load, on a mass basis, is retained in the lung at 56 days after exposure for both particles. This suggests that there is a portion of silver that is located in a region of the lung not readily cleared by macrophages and is not dependent on particle size.

We constructed and characterized a system to create an atmosphere of AgNPs to assess the deposition and retention of the nanoparticles in the lung following a nose-only inhalation exposure. Because the AgNPs supplied by the NCNHIR were in a liquid suspension, it was necessary to use a system that could

Downloaded from http://toxsci.oxfordjournals.org/ at Government on August 9, 2016

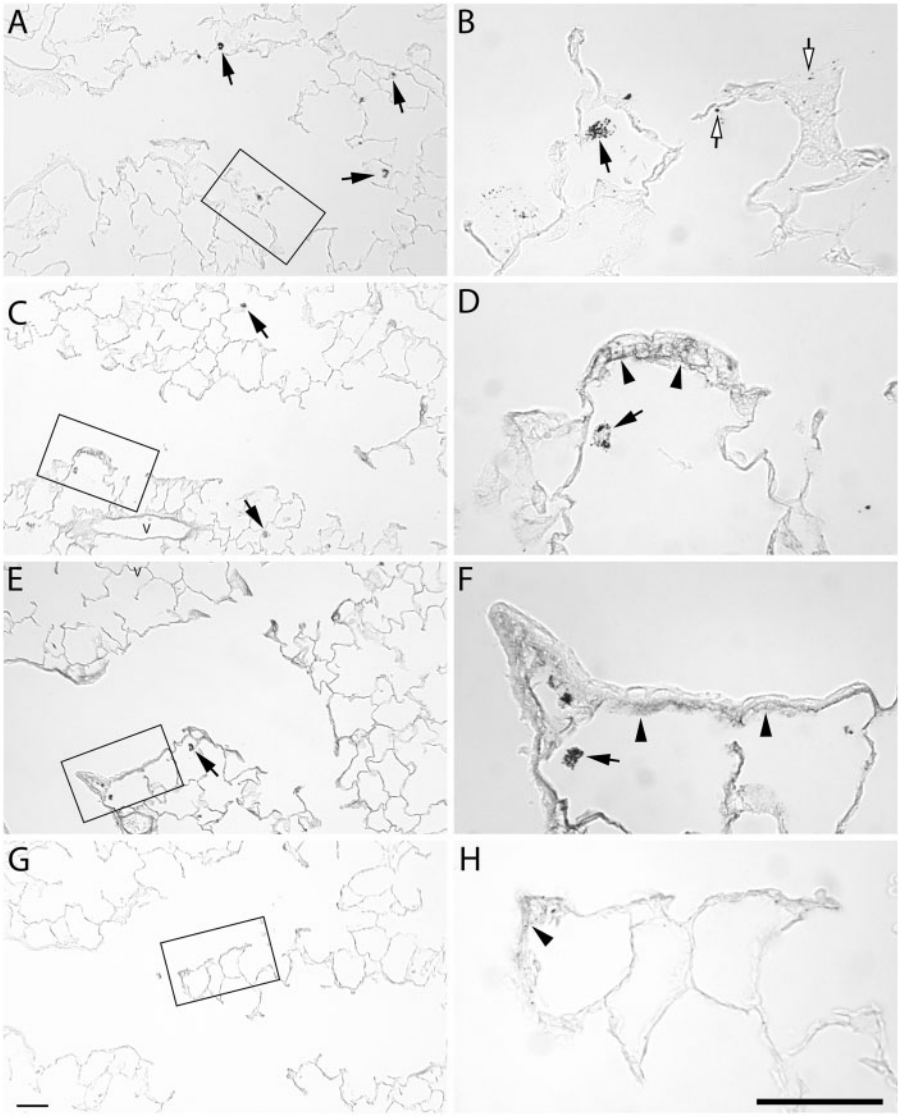


FIG. 6. Autometallography of silver localization from 20 nm AgNP at the alveolar duct junction. Lung tissue stained for silver at 1 day (A, B), 7 days (C, D), 21 days (E, F), and 56 days (G, H) post-exposure to aerosolized 20 nm AgNP. Silver positive macrophages (arrows) were detected at 1, 7, and 21 days. Deposition to the epithelium (open arrows) at 1 day. Staining of the subepithelial basement membrane zone is observed at 7 and 21 days, and to a lesser extent at 56 days (arrowheads). Bars = 50 μm.

aerosolize such a material and subsequently dry the aerosol removing water. This is in contrast to Roberts *et al.* (2013) which administered a wet aerosol of uncoated AgNPs and found little effect in lung tissue. Our current study produced an exposure dose that was similar to that administered in a previous intratracheal dose response study (0.5–1.0 mg/kg) (Anderson *et al.*, 2014), which was based on a maximal human exposure of 289 μg/m$^3$ for 1 month (8 h per day, 5 days per week) (Wang *et al.*, 2014). The delivered dose following aerosol exposure was estimated to be 0.23 and 0.17 mg/kg for 20 and 110 nm AgNPs, respectively, based on an average animal weight at time of exposure of 355 g.

In our previous study instilling the same AgNPs, we saw no significant clearance of silver from the lung of either size at up to 21 days post-treatment (Anderson *et al.*, 2014). However, in this study we found approximately 60% of silver from either size AgNP was cleared from the lung at 21 days post-exposure. In a study by Takenaka *et al.* (2001) exposing rats for 6 h to 15 nm uncoated AgNP, there was 62% clearance 24 h after exposure and almost 96% by 7 days. However, the exposure concentration, 133 μg/m$^3$, was much lower than this study (see Table 1). Kwon *et al.* (2012) exposed mice to 20 nm uncoated AgNP at a concentration of 2.9 mg/m$^3$, and observed a 24-h clearance of 76%. Their rates are considerably higher than the 14% and 24% 24 h clearance rates measured in this study for the 20 and 110 nm AgNPs, respectively. It must be noted that these studies used uncoated AgNPs. We have observed instilled 20 nm polyvinylpyrrolidone (PVP)-coated AgNPs having significantly greater clearance than 20 nm citrate-coated AgNPs (Anderson *et al.*, 2014). A recent study using uncoated 15 nm AgNP and PVP-coated 410 nm Ag particles inhaled by rats saw a difference in the 2 particle sizes. Clearance was assessed between 1 day and 7 days post-exposure and the was 62% clearance of the 15 nm particles, but only 31% clearance of the 410 nm particles (Braakhuis *et al.*, 2014). We found that the 1–7 day clearance was 34% and 24% for the 20 and 110 nm particles, respectively.

Downloaded from http://toxsci.oxfordjournals.org/ at Government on August 9, 2016

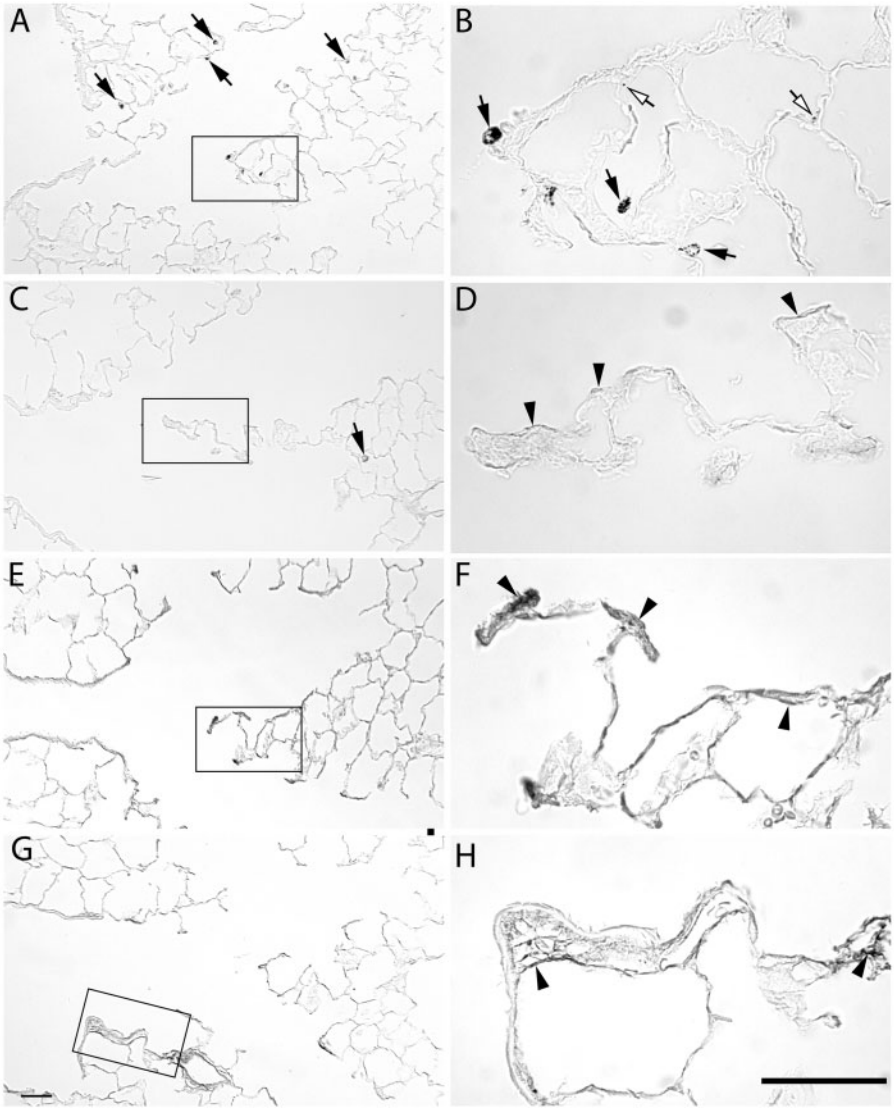


FIG. 7. Autometallography of silver localization from 110 nm AgNP at the alveolar duct junction. Lung tissue stained for silver at 1 day (A, B), 7 days (C, D), 21 days (E, F), and 56 days (G, H) post-exposure to aerosolized 110 nm AgNP. Silver positive macrophages (arrows) are detected at 1, 7, and 21 day timepoints. Silver localized to the epithelium (open arrows) at 1 day. Staining of the subepithelial basement membrane zone is observed at 7 and 21 days, and to a lesser level at 56 days (arrowheads). Bars = 50 μm.

Indicating that larger particles have less clearance during this time period in both studies and that particles of similar sizes had similar clearance in both studies. Of note is that the Braakhuis *et al*. study was a 4 consecutive day study with exposures for 6 h/day. Comparing the limited number of aerosol silver exposure studies is problematic due to differences in exposure levels, particle size, and surface coatings, as well as mechanism of aerosol generation.

Macrophages are critical to pulmonary particle clearance (Geiser *et al*., 2008; Geiser, 2010; Oberdorster *et al*., 1992). The predominant lung cell type containing silver is the macrophage and our data indicate that AgNPs persist in macrophages even 56 days after exposure. Some concern might be that neutrophils are contributing to silver clearance in our exposure model. While there was not an increase in BALF neutrophils at 1 day post-exposure, there was a significant increase in BALF neutrophils at 7 days (data not shown; manuscript in preparation). However, neutrophils did not contain silver staining at any timepoint examined and so did not contribute to particle clearance in this model. At 1 day post-exposure when there was heavy involvement of macrophages with particle scavenging and clearance, more than half of the recovered macrophages were positive for silver irrespective of the particle size. However, there was not an increase in non-viable BALF cells, indicating that the silver did not cause toxicity to the macrophages. This is in contrast to other studies which suggest that macrophage ingestion of AgNPs results in cytotoxicity to the macrophage, possibly due to Ag ion release (Singh and Ramarao, 2012). However, it is possible that macrophages with a cytotoxic response were already removed from the lung via the mucociliary escalator. In a previous study where the same particles were administered intratracheally, there was either an increase or no change in the number or macrophages recovered in BALF, and no difference in the number of non-viable cells in BALF (Anderson *et al*., 2014). This is in contrast to the current aerosol exposure study that found a significant decrease in BALF macrophages 1 day post-exposure compared with controls. One explanation is that macrophages resident in the lung,

Downloaded from http://toxsci.oxfordjournals.org/ at Government on August 9, 2016

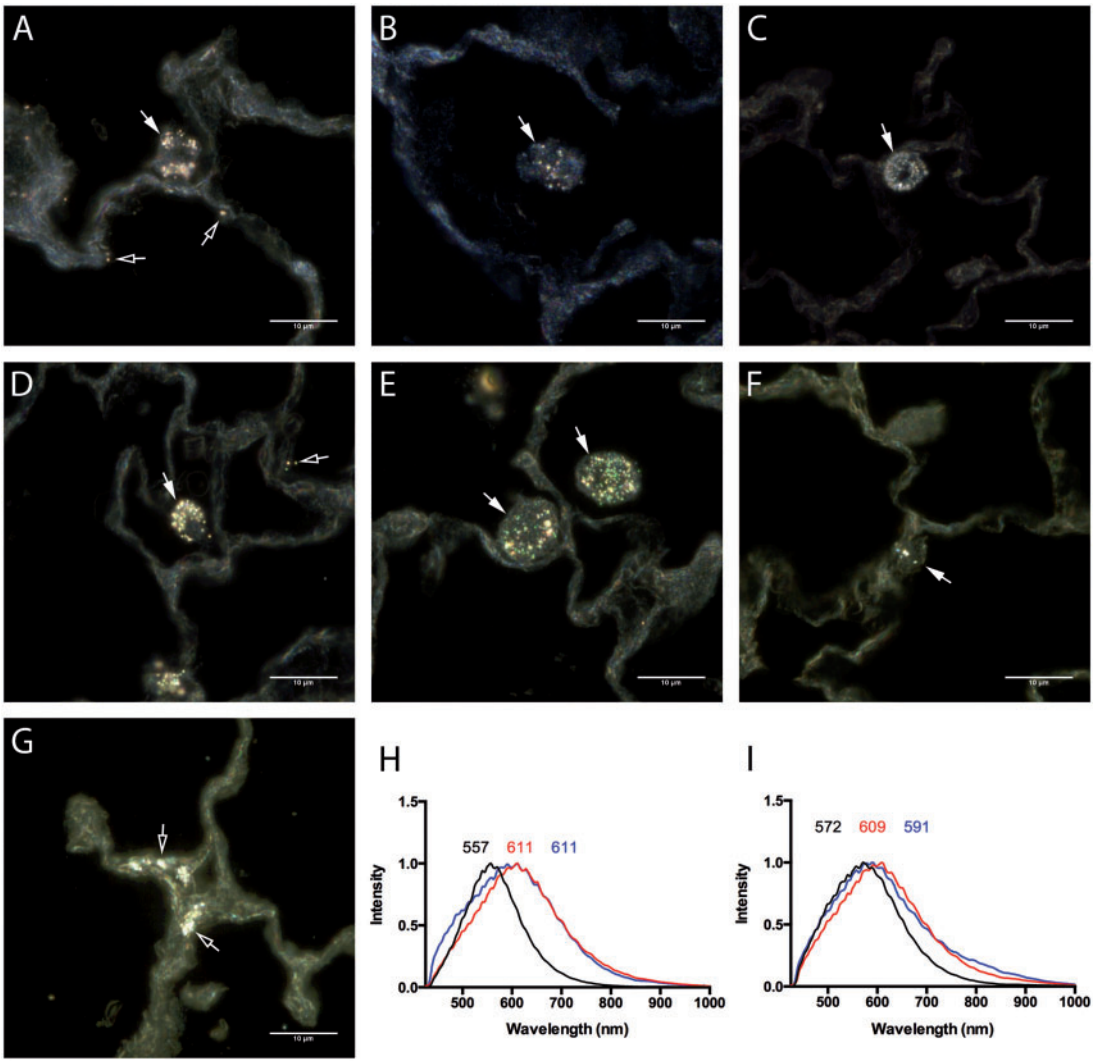


FIG. 8. Cytoviva-enhanced dark field images of AgNPs in unstained paraffin embedded lung sections. Cellular AgNPs uptake within the lung was qualitatively evaluated by the assessment of lung sections following exposure to 20 nm AgNP at (A) 1 day, (B) 7 days, and (C) 21 days or 110 nm AgNP at (D) 1 day, (E) 7 days, and (F) 21 days by Cytoviva-enhanced dark field microscopy. (G) AgNPs within lung epithelial cells at 21 days following exposure to 20 nm AgNP. Alterations in mean spectral profiles for (H) 20 nm AgNP and (I) 110 nm AgNP. Mean spectral profiles of AgNPs (black), AgNPs within alveolar macrophages at 24 h (red), and following 24 h incubation with artificial lysosomal fluid (ALF) (blue). Bar = 10 μm.

having scavenged silver, are being removed at a faster rate following inhalation exposure and they are removed faster than they can be replaced in the first 24 h. Macrophage populations can include both resident and recruited macrophages and these have a 30-day long half-life in rodents (Murphy *et al.*, 2008). Thus, it is not possible to determine whether the macrophages that contain the silver at various timepoints, scavenged it recently or some time ago.

In regards to the percentage of silver positive macrophages present following intratracheal administration, both AgNPs produced less than 40% silver positive macrophages at doses up to 1 mg/kg (>300 μg/rat). However, in the current inhalation exposure study there were greater than 50% silver positive macrophages at 1 day post-exposure (Fig. 4B). This suggests that the diffuse distribution of silver following inhalation exposure involves more initial macrophages than a higher intratracheally administered dose. The macrophage silver scores from this study and previous work using intratracheal instillation indicates more involvement in scavenging the smaller particles; scores for macrophages recovered from animals exposed to 20 versus 110 nm AgNPs are higher at 1 day post-exposure. This difference in macrophage response to inhalation of different size particles is interesting because the SMPS data indicate there is only a small difference in the size of the aerosolized particles. The 20 nm AgNP form aggregates and one possibility is that the microstructure of these agglomerates is sensed differently by the macrophages. Another possibility is that the agglomerates of 20 nm AgNP disassemble upon contact with the lung lining fluid and are presented to macrophages in their original size and the macrophages are less efficient at removing these smaller particles. The higher number of smaller particles may also contribute to less efficient clearance. As noted in other studies of macrophages that phagocytose AgNPs, a variety of macrophage profiles were present including those that contained compact agglomerates of varying degrees (Wang *et al.*, 2012).

Macrophage-mediated clearance is not the only mechanism for silver removal from the lung tissue. For particles in the

Downloaded from http://toxsci.oxfordjournals.org/ at Government on August 9, 2016

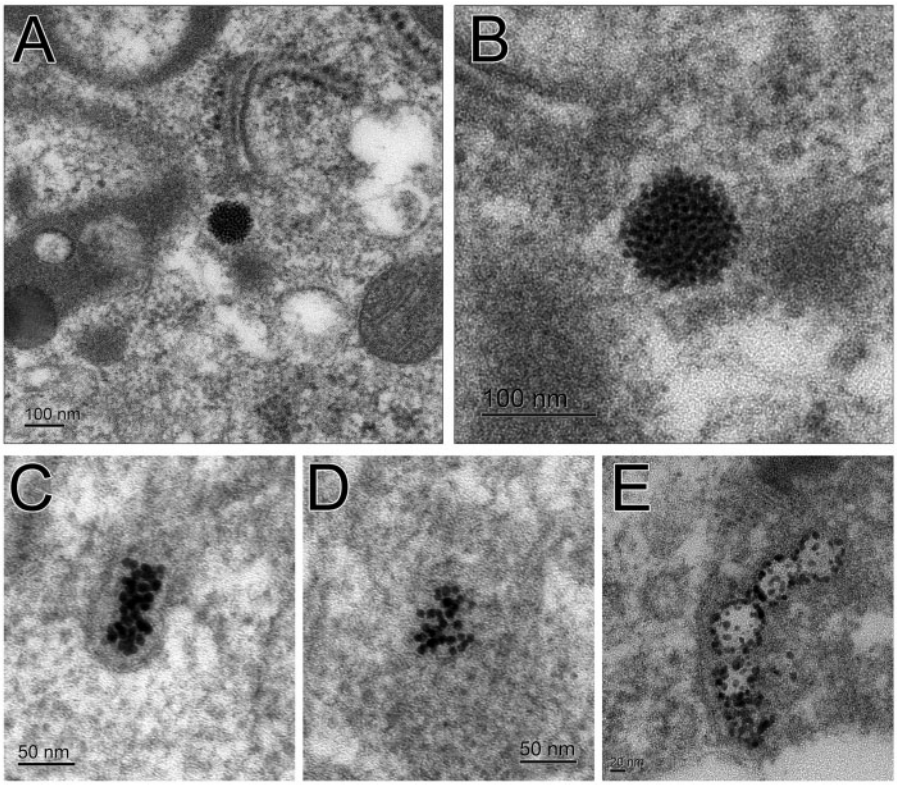


FIG. 9. TEM images of AgNPs in BALF macrophages. Small silver particles have clumped together to form a larger spherical particle from the original 20 nm AgNP (A, B). Lesser number of the smaller particles from the original 20 nm AgNP are less organized (C, D). Small particles from the original 110 nm AgNP are along the membrane of a vesicle (E).

nanosize range, and for silver in particular, other options are translocation of the particle itself or partial dissolution of the AgNPs. Silver shed by AgNPs, as free ions or bound to other molecules, could move out of the lung, and this has been reported for intranasally instilled AgNPs (Genter *et al.*, 2012). Further, *in vitro* studies using silver particles from various sources have suggested that smaller particles shed more ions than larger particles and this may contribute to their toxicity (Gliga *et al.*, 2014). We note that very low levels of particle dissolution *in vitro* have been noted for the particles used in this study with a dissolution of 4.3% for the 20 nm particles and 2.2% for the 110 nm particles after 24 h in bronchial epithelial growth medium (BEGM) (Wang *et al.*, 2014). However, studies of citrate-coated AgNPs in lung surfactant have shown that lung lining fluid can affect the aggregation state and release of $Ag+$ ions in the lung (Leo *et al.*, 2013), so the form of the AgNPs over time *in vivo* is still an open question. While our current study did not determine the form of the silver remaining in the lung over time, the presence of smaller AgNPs found in the TEM images of BALF macrophages (Fig. 9) suggests that the AgNP may be not just releasing ions, but also may be forming secondary particles. Work by our group has shown, using x-ray absorption spectroscopy, that while the particles had changed in form by 7 days post-exposure, the predominant silver species was metallic silver and not silver ions (Davidson *et al.*, 2014). Measuring the translocation of silver and silver ions to other organs may be a fruitful avenue for a future study.

The pattern of silver localization in lung tissue was similar between both particle sizes (Figs. 6 and 7) with staining of silver predominantly in the terminal bronchial/alveolar duct junction and in macrophages. Through the use of hyperspectral analysis, we determined that AgNPs internalized by macrophages underwent a red shift in spectrum which is often indicative of the association of biomolecules on the particle surface. In an attempt to identify the likely subcellular localization of AgNPs within macrophages, AgNPs were acellularly incubated in ALF that has a composition and pH similar to intracellular phagolysosomal conditions. AgNPs incubated in ALF demonstrated a spectral profile similar to the AgNPs internalized within macrophages indicative of AgNPs accumulation within phagolysosomal compartments of the macrophages. While these changes in spectra are suggestive of subcellular localization of AgNPs into the phagolysosome, *in vitro* studies of other metal nanoparticles such as zinc oxide have demonstrated this as a common site of accumulation within macrophages (Xia *et al.*, 2008) and our TEM data support this outcome. One day after exposure, the silver localization was very diffuse in the tissue, suggesting that the aerosolized AgNPs were spread widely in the distal regions of the lung. There was little silver staining in proximal airways even at early timepoints, yet there was measured silver even in the trachea by ICP-MS due to the great sensitivity of this technique. Disparities in detection between methods may be due to processing as the tissues used for histology were fixed by inflating with liquid fixative that could flush macrophages and AgNPs deeper into the lung, while ICP-MS samples were flash frozen. Our study confirms other studies (Kwon *et al.*, 2012; *Roberts et al.*, 2013; Stebounova *et al.*, 2011) that show acute frank lung toxicity was not present following exposure to AgNPs as epithelial cells were not detected in the BALF and tissue morphology had a regular appearance. However, further studies should be conducted to determine whether any abnormal pathologies, changes in lung function or signaling molecules are present as these have been reported for other studies of

Downloaded from http://toxsci.oxfordjournals.org/ at Government on August 9, 2016

AgNPs (Kwon *et al.*, 2012; Song *et al.*, 2013; Wang *et al.*, 2014), particularly since the 20 nm particles are very persistent in the lung tissue.

While the most prominent localization of silver in the tissues occurred within macrophages, interstitial localization, as well as intraepithelial localization (Figs. 6–8) of the silver in lung tissue was noted at 1 and 7 days following exposure. In previous work with ultrafine particles (Oberdorster *et al.*, 1992), it was hypothesized that this sort of "interstitialization", that results in retention in the tissue itself, would depend on the size of the particle and the degree of particle lung burden, with smaller particles and higher doses having a greater effect. In the current study, both particles were ultrafine but the 20 nm particles had a greater localization to the subepithelial basement membrane zone than the 110 nm particles. However, this could also reflect increased total particle number. Previous *in vitro* studies using the A549 lung epithelial cell line have shown uptake of AgNPs by lung cells into both the cytosol and the nucleus, with little cytotoxicity (Cronholm *et al.*, 2013; Herzog *et al.*, 2013). Oral administration of AgNPs also results in silver localization in the gut particularly in the lamina propria and in macrophages, but not in the gut epithelial cytoplasm (Loeschner *et al.*, 2011). Accumulation of AgNPs in extracellular spaces is also supported by studies in the liver (Su *et al.*, 2014).

MPPD modeling software was used in this study to estimate a deposited dose to allow comparisons to other methods of exposure, such as intratracheal instillation. Using the MPPD model to calculate the delivered dose of AgNPs to the lower respiratory system and the mean body weight of the exposed rats, we estimate the inhaled delivered dose for this study to be 80 and 59 μg for the 20 and 110 nm AgNPs, respectively. However, the $T_0$ ICP-MS measurements of silver in the rat lung detected only 321 (20 nm AgNP) and 357 ng (110 nm AgNP) over the entire thoracic respiratory system (the 5 lung lobe, trachea, and lobar bronchus summed). This can be primarily attributed to only a fraction of the generated aerosol getting to the respiratory region of the lung. The cascade impactor data indicate that large agglomerates of particles are formed. While these particles are a small number fraction of the total particles, they represent a large fraction of the mass of particles generated. The large particles are removed from the airflow in the nasal cavity and would not be deposited in the lung. Nasal cavity is important to the study of these aerosolized particles and this will be addressed in future studies. Strain-specific effects on deposition could also contribute to the observed differences between the calculated values and the measured values for deposition. The version 2.11 of the MPPD software uses lung structure data for the Long-Evans rat, while the Sprague Dawley rat was used in this study. A recent study in mice showed that strain differences could affect deposition of particles in the lung (Asgharian *et al.*, 2014). Another factor that can contribute to differential calculated values versus $T_0$ measurements is exposure duration. Inhalation exposure studies do not instantly deliver the particles. Clearance of particles should begin as particles are deposited in the lung during the exposure, so particles deposited early have time to be cleared before the exposure ends. Finally, the MPPD model assumes particles are insoluble (Asgharian *et al.*, 2001a,b) but AgNPs are slightly soluble (Behra *et al.*, 2013; Danscher and Locht, 2010; Stebounova *et al.*, 2011; Wang *et al.*, 2014). The MPPD model predicts 34.8% of 20 nm and 31.7% of 110 nm nanoparticles will still be retained in the lung at 56 days. This is in close agreement with the percentage of silver measured by ICP-MS, 33% and 35% for 20 and 110 nm AgNPs, respectively.

In conclusion, our study shows that inhalation of both 20 or 110 nm AgNPs resulted in a persistence of silver in the lung at 56 days post-exposure, with greater than 30% retained silver from both particle sizes. We also observed a difference in both the number of, and the silver burden in, BALF macrophages, with 20 nm AgNP producing a greater load of silver positive macrophages shortly after exposure (1 day) and a greater number of low burden macrophages at later timepoints (21 and 56 days). Additionally, we saw evidence of silver being retained in lung tissue in the terminal bronchiole/alveolar duct junction region of the lung regardless of particle size. This current study supports that particle size affects macrophage clearance, but has little effect on long-term retention of silver in the lung.

## SUPPLEMENTARY DATA

Supplementary data are available online at http://toxsci.oxfordjournals.org/.

## ACKNOWLEDGMENTS

The authors are grateful to the following people for their skilled technical assistance during sample collection and processing: Patricia Edwards, Ryan Mendoza, Imelda Espiritu, and Janice Peake. Imaging was conducted at the UC Davis Cellular and Molecular Imaging core. They thank the UC Davis Interdisciplinary Center for Inductively Coupled Plasma Mass Spectrometry and both Peter Green and Joel Commisso for assistance with the ICP-MS samples and analysis. They thank the UC Davis Electron Microscopy Laboratory, Department of Medical Pathology and Laboratory Medicine, School of Medicine and Patricia Kysar for assistance with the macrophage TEM images. They thank Ian Kennedy for the use of the SMPS and Chris Wallis for his instruction in operating the SMPS.

## FUNDING

Grant support (U01 ES020127, U01 ES020126, and U19 ES019525) and silver nanomaterials used in this study where procured, characterized, and provided to investigators by NCNHIR Consortium. We acknowledge a Superfund Research Program Fellowship in support of D.S.A. (P42 ES004699), the NIH National Heart, Lung and Blood Institute T32 Training Program (T32 HL086350) for E.S.P., and the Western Center for Agricultural Health and Safety (NIOSH Grant 0H07550) for R.M.S. The NCNHIR was established with the centers funded by RFA ES-09-011. These centers formed a consortium with other NIEHS-funded researchers and other federal laboratories in the area of Nano EHS and worked together on a select set of engineered nanomaterials provided to the consortium by NIEHS. Any opinions, findings, conclusions, or recommendations expressed herein are those of the author(s) and do not necessarily reflect the views of the National Institute of Environmental Health Sciences/NIH.

## REFERENCES

Anderson, D. S., Silva, R. M., Lee, D., Edwards, P. C., Sharmah, A., Guo, T., Pinkerton, K. E., and Van Winkle, L. S. (2014). Persistence of silver nanoparticles in the rat lung: influence

Downloaded from http://toxsci.oxfordjournals.org/ at Government on August 9, 2016

of dose, size and chemical composition. *Nanotoxicology* **18,** 1–12.

Asgharian, B., Hofman, W., and Bergmann, R. (2001a). Particle deposition in a multiple-path model of the human lung. *Aerosol Sci. Technol.* **34,** 332–339.

Asgharian, B., Hofmann, W., and Miller, F. J. (2001b). Mucociliary clearance of insoluble particles from the tracheobronchial airways of the human lung. *J. Aerosol Sci.* **32,** 817–832.

Asgharian, B., Price, O. T., Oldham, M., Chen, L. C., Saunders, E. L., Gordon, T., Mikheev, V. B., Minard, K. R., and Teeguarden, J. G. (2014). Computational modeling of nanoscale and microscale particle deposition, retention and dosimetry in the mouse respiratory tract. *Inhal. Toxicol.* **26,** 829–842.

Behra, R., Sigg, L., Clift, M. J., Herzog, F., Minghetti, M., Johnston, B., Petri-Fink, A., and Rothen-Rutishauser, B. (2013). Bioavailability of silver nanoparticles and ions: from a chemical and biochemical perspective. *J. R. Soc. Interface* **10,** 20130396.

Braakhuis, H. M., Gosens, I., Krystek, P., Boere, J., Cassee, F. R., Fokkens, P., Post, J., van Loveren, H., and Park, M. (2014). Particle size dependent deposition and pulmonary inflammation after short-term inhalation of silver nanoparticles. *Part. Fibre Toxicol.* **11,** 49.

Cronholm, P., Karlsson, H. L., Hedberg, J., Lowe, T. A., Winnberg, L., Elihn, K., Wallinder, I. O., and Moller, L. (2013). Intracellular uptake and toxicity of Ag and CuO nanoparticles: a comparison between nanoparticles and their corresponding metal ions. *Small* **9,** 970–982.

Danscher, G., and Locht, L. J. (2010). In vivo liberation of silver ions from metallic silver surfaces. *Histochem. Cell Biol.* **133,** 359–366.

Danscher, G., and Stoltenberg, M. (2006). Silver enhancement of quantum dots resulting from (1) metabolism of toxic metals in animals and humans, (2) in vivo, in vitro and immersion created zinc-sulphur/zinc-selenium nanocrystals, (3) metal ions liberated from metal implants and particles. *Prog. Histochem. Cytochem.* **41,** 57–139.

Davidson, R. A., Anderson, D. S., Van Winkle, L. S., Pinkerton, K. E., and Guo, T. (2015). Evolution of silver nanoparticles in the rat lung investigated by X-ray absorption spectroscopy. *J. Phys. Chem. A* **119,** 281–289.

Geiser, M. (2010). Update on macrophage clearance of inhaled micro- and nanoparticles. *J. Aerosol Med. Pulm. Drug Deliv.* **23,** 207–217.

Geiser, M., Casaulta, M., Kupferschmid, B., Schulz, H., Semmler-Behnke, M., and Kreyling, W. (2008). The role of macrophages in the clearance of inhaled ultrafine titanium dioxide particles. *Am. J. Respir. Cell Mol. Biol.* **38,** 371–376.

Genter, M. B., Newman, N. C., Shertzer, H. G., Ali, S. F., and Bolon, B. (2012). Distribution and systemic effects of intranasally administered 25 nm silver nanoparticles in adult mice. *Toxicol. Pathol.* **40,** 1004–1013.

Gliga, A. R., Skoglund, S., Wallinder, I. O., Fadeel, B., and Karlsson, H. L. (2014). Size-dependent cytotoxicity of silver nanoparticles in human lung cells: the role of cellular uptake, agglomeration and Ag release. *Part. Fibre Toxicol.* **11,** 11.

Glover, R. D., Miller, J. M., and Hutchison, J. E. (2011). Generation of metal nanoparticles from silver and copper objects: nanoparticle dynamics on surfaces and potential sources of nanoparticles in the environment. *ACS Nano.* **5,** 8950–8957.

Hacker, G. W., Grimelius, L., Danscher, G., Bernatzky, G., Muss, W., Adam, H., and Thurner, J. (1988). Silver acetate autometallography—an alternative enhancement technique for immunogold-silver staining (IGSS) and silver amplification of gold, silver, mercury and zinc in tissues. *J. Histotechnol.* **11,** 213–221.

Herzog, F., Clift, M. J., Piccapietra, F., Behra, R., Schmid, O., Petri-Fink, A., and Rothen-Rutishauser, B. (2013). Exposure of silver-nanoparticles and silver-ions to lung cells in vitro at the air-liquid interface. *Part. Fibre Toxicol.* **10,** 11.

Hindi, K. M., Ditto, A. J., Panzner, M. J., Medvetz, D. A., Han, D. S., Hovis, C. E., Hilliard, J. K., Taylor, J. B., Yun, Y. H., Cannon, C. L., and Youngs, W. J. (2009). The antimicrobial efficacy of sustained release silver-carbene complex-loaded L-tyrosine polyphosphate nanoparticles: characterization, in vitro and in vivo studies. *Biomaterials* **30,** 3771–3779.

Jang, S., Park, J. W., Cha, H. R., Jung, S. Y., Lee, J. E., Jung, S. S., Kim, J. O., Kim, S. Y., Lee, C. S., and Park, H. S. (2012). Silver nanoparticles modify VEGF signaling pathway and mucus hypersecretion in allergic airway inflammation. *Int. J. Nanomed.* **7,** 1329–1343.

Ji, J. H., and Yu, I. J. (2012). Estimation of human equivalent exposure from rat inhalation toxicity study of silver nanoparticles using multi-path particle dosimetry model. Toxicol. Res. **1,** 206–210.

Ji, J. H., Jung, J. H., Kim, S. S., Yoon, J. U., Park, J. D., Choi, B. S., Chung, Y. H., Kwon, I. H., Jeong, J., Han, B. S., *et al.* (2007). Twenty-eight-day inhalation toxicity study of silver nanoparticles in Sprague-Dawley rats. *Inhal. Toxicol.* **19,** 857–871.

Kwon, J. T., Minai-Tehrani, A., Hwang, S. K., Kim, J. E., Shin, J. Y., Yu, K. N., Chang, S. H., Kim, D. S., Kwon, Y. T., Choi, I. J., *et al.* (2012). Acute pulmonary toxicity and body distribution of inhaled metallic silver nanoparticles. *Toxicol. Res.* **28,** 25–31.

Lee, J., Ahn, K., Kim, S., Jeon, K., Lee, J., and Yu, I. (2012). Continuous 3-day exposure assessment of workplace manufacturing silver nanoparticles. *J. Nanopart. Res.* **14,** 1134.

Leo, B. F., Chen, S., Kyo, Y., Herpoldt, K. L., Terrill, N. J., Dunlop, I. E., McPhail, D. S., Shaffer, M. S., Schwander, S., Gow, A., *et al.* (2013). The stability of silver nanoparticles in a model of pulmonary surfactant. *Environ. Sci. Technol.* **47,** 11232–11240.

Levard, C., Hotze, E. M., Lowry, G. V., and Brown, G. E. (2012). Environmental transformations of silver nanoparticles: impact on stability and toxicity. *Environ. Sci. Technol.* **46,** 6900–6914.

Loeschner, K., Hadrup, N., Qvortrup, K., Larsen, A., Gao, X., Vogel, U., Mortensen, A., Lam, H. R., and Larsen, E. H. (2011). Distribution of silver in rats following 28 days of repeated oral exposure to silver nanoparticles or silver acetate. *Part. Fibre Toxicol.* **8,** 18.

Londahl, J., Moller, W., Pagels, J. H., Kreyling, W. G., Swietlicki, E., and Schmid, O. (2014). Measurement techniques for respiratory tract deposition of airborne nanoparticles: a critical review. *J. Aerosol Med. Pulm. Drug Deliv.* **27,** 229–254.

Marchiol, L., Mattiello, A., Poscic, F., Giordano, C., and Musetti, R. (2014). In vivo synthesis of nanomaterials in plants: location of silver nanoparticles and plant metabolism. *Nanoscale Res. Lett.* **9,** 101.

Murphy, J., Summer, R., Wilson, A. A., Kotton, D. N., and Fine, A. (2008). The prolonged life-span of alveolar macrophages. *Am. J. Respir. Cell Mol. Biol.* **38,** 380–385.

The Project of Emerging Nanotechnologies. (2014). This is the first publicly available on-line inventory of nanotechnology-based consumer products. In *Consumer Products Inventory*, 2014 ed. Woodrow Wilson International Center for Scholars, Washington, DC. Retrieved from http://www.nanotechproject.org/cpi. Accessed March 30, 2014.

Oberdorster, G., Ferin, J., and Lehnert, B. E. (1994). Correlation between particle size, in vivo particle persistence, and lung injury. *Environ. Health Perspect.* **102,** (Suppl. 5), 173–179.

Downloaded from http://toxsci.oxfordjournals.org/ at Government on August 9, 2016

Oberdorster, G., Ferin, J., Gelein, R., Soderholm, S. C., and Finkelstein, J. (1992). Role of the alveolar macrophage in lung injury: studies with ultrafine particles. *Environ. Health Perspect.* **97,** 193–199.

Pelgrift, R. Y., and Friedman, A. J. (2013). Nanotechnology as a therapeutic tool to combat microbial resistance. *Adv. Drug Deliv. Rev.* **65,** 1803–1815.

Raabe, O. G. (1979). Design and use of the Mercer-style impactor for characterization of aerosol aerodynamic size distributions. In Lundgren, D. A. (ed) *Aerosol Measurements*, pp. 135–140. University Presses of Florida, Gainesville, FL.

Raabe, O. G., Bennick, J. E., Light, M. E., Hobbs, C. H., Thomas, R. L., and Tillery, M. I. (1973). An improved apparatus for acute inhalation exposure of rodents to radioactive aerosols. *Toxicol. Appl. Pharmacol.* **26,** 264–273.

Roberts, J. R., McKinney, W., Kan, H., Krajnak, K., Frazer, D. G., Thomas, T. A., Waugh, S., Kenyon, A., MacCuspie, R. I., Hackley, V. A., and Castranova, V. (2013). Pulmonary and cardiovascular responses of rats to inhalation of silver nanoparticles. *J. Toxicol. Environ. Health A* **76,** 651–668.

Schmoll, L. H., Elzey, S., Grassian, V. H., and O'Shaughnessy, P. T. (2009). Nanoparticle aerosol generation methods from bulk powders for inhalation exposure studies. *Nanotoxicology* **3,** 265–275.

Singh, R. P., and Ramarao, P. (2012). Cellular uptake, intracellular trafficking and cytotoxicity of silver nanoparticles. *Toxicol. Lett.* **213,** 249–259.

Smith, D. R., and Fickett, F. R. (1995). Low-temperature properties of silver. *J. Res. Natl. Inst. Stand. Technol.* **100,** 119–171.

Song, K. S., Sung, J. H., Ji, J. H., Lee, J. H., Lee, J. S., Ryu, H. R., Lee, J. K., Chung, Y. H., Park, H. M., Shin, B. S., *et al.* (2013). Recovery from silver-nanoparticle-exposure-induced lung inflammation and lung function changes in Sprague Dawley rats. *Nanotoxicology* **7,** 169–180.

Stebounova, L. V., Adamcakova-Dodd, A., Kim, J. S., Park, H., O'Shaughnessy, P. T., Grassian, V. H., and Thorne, P. S. (2011). Nanosilver induces minimal lung toxicity or inflammation in a subacute murine inhalation model. *Part. Fibre Toxicol.* **8,** 5.

Su, C. K., Hung, C. W., and Sun, Y. C. (2014). In vivo measurement of extravasation of silver nanoparticles into liver extracellular space by push-pull-based continuous monitoring system. *Toxicol. Lett.* **227,** 84–90.

Sung, J. H., Ji, J. H., Park, J. D., Yoon, J. U., Kim, D. S., Jeon, K. S., Song, M. Y., Jeong, J., Han, B. S., Han, J. H., *et al.* (2009). Subchronic inhalation toxicity of silver nanoparticles. *Toxicol. Sci.* **108,** 452–461.

Sung, J. H., Ji, J. H., Yoon, J. U., Kim, D. S., Song, M. Y., Jeong, J., Han, B. S., Han, J. H., Chung, Y. H., Kim, J., *et al.* (2008). Lung function changes in Sprague-Dawley rats after prolonged inhalation exposure to silver nanoparticles. *Inhal. Toxicol.* **20,** 567–574.

Takenaka, S., Karg, E., Roth, C., Schulz, H., Ziesenis, A., Heinzmann, U., Schramel, P., and Heyder, J. (2001). Pulmonary and systemic distribution of inhaled ultrafine silver particles in rats. *Environ. Health Perspect.* **109**, (Suppl. 4), 547–551.

Van Winkle, L. S., Buckpitt, A. R., Nishio, S. J., Isaac, J. M., and Plopper, C. G. (1995). Cellular response in naphthalene-induced Clara cell injury and bronchiolar epithelial repair in mice. *Am. J. Physiol.* **269**, (Pt 1), L800–L818.

Wang, H., Wu, L., and Reinhard, B. M. (2012). Scavenger receptor mediated endocytosis of silver nanoparticles into J774A.1 macrophages is heterogeneous. *ACS Nano.* **6,** 7122–7132.

Wang, X., Ji, Z., Chang, C. H., Zhang, H., Wang, M., Liao, Y. P., Lin, S., Meng, H., Li, R., Sun, B., *et al.* (2014). Use of coated silver nanoparticles to understand the relationship of particle dissolution and bioavailability to cell and lung toxicological potential. *Small* **10,** 385–398.

Xia, T., Kovochich, M., Liong, M., Mädler, L., Gilbert, B., Shi, H., Yeh, J. I., Zink, J. I., and Nel, A. E. (2008). Comparison of the mechanism of toxicity of zinc oxide and cerium oxide nanoparticles based on dissolution and oxidative stress properties. *ACS Nano* **2,** 2121–2134.

Xiang, D., Zheng, Y., Duan, W., Li, X., Yin, J., Shigdar, S., O'Connor, M. L., Marappan, M., Zhao, X., Miao, Y., *et al.* (2013). Inhibition of A/Human/Hubei/3/2005 (H3N2) influenza virus infection by silver nanoparticles in vitro and in vivo. *Int. J. Nanomed.* **8,** 4103–4113.

Downloaded from http://toxsci.oxfordjournals.org/ at Government on August 9, 2016